**FLUCOME 2009**

**10th International Conference on Fluid Control, Measurements, and Visualization**
**August 17–21, 2009, Moscow, Russia**

# AERODYNAMIC RESPONSE OF AN EMS-TYPE MAGLEV VEHICLE RUNNING ON FLEXIBLE GUIDEWAYS

J.D. Yau [1]

**ABSTRACT**

In this paper, an incremental iterative procedure was carried out to study aerodynamic response of an EMS-type maglev vehicle moving over a series of guideway girders at constant speeds. The maglev vehicle is simulated as a rigid car body supported by a rigid levitation frame using a uniformly distributed spring-dashpot system, in which the electromagnetic forces are controlled by an on-board optimal PI controller and the guideway unit is modeled as a series of simple beams with identical span. Considering the motion-dependent nature of electromagnetic forces and the velocity-dependent characteristics of aerodynamic forces, this study presents an iterative approach in conjunction with the simulation of aerodynamic coefficient curves approximated by a number of *piecewise connected linear segments* through subdivision to compute the interaction response of the maglev vehicle/guideway coupling system. Numerical simulations demonstrate that the aerodynamic forces lead to a significant amplification on the acceleration amplitude of the running maglev vehicle at higher speeds. Such an aerodynamic phenomenon should be taken into account in the analysis and design stage of a maglev transport system.

**Keywords: Aerodynamics; guideway; maglev vehicle; PI controller; vibration.**

## INTRODUCTION

Successful operating experience of the Shanghai Maglev transport system since 2002 marked a new era in commercial maglev transport system. Compared with traditional trains with wheel/track contact mode, Maglev transport system can offer many advantages, such as low energy consumption, less environmental impact, as well as lower noise and emissions. Moreover, the powerful magnets under modern maglev technology are able to lift a vehicle up and propel it forward along a guideway via electromagnetic forces. According to the suspension modes, two kinds of maglev technologies have been developed: (1) electromagnetic suspension (EMS) with attractive mode; (2) electrodynamic suspension (EDS) with repulsive mode (Bittar and Sales, 1998; Yau, 2009). The EMS system can lift a vehicle up using attractive forces by the magnets beneath a guide-rail. The EDS system takes the vehicle above its guide-rail in the U-shaped guideway by using magnetic repulsive forces. To suspend a maglev vehicle at a stable levitation gap (air gap) between the on-board levitation magnets and the guideway, a controllable electromagnetic field is generated in its maglev suspension system. Generally, the EDS system can suspend a train above its guide-rail using *concentrated* magnetic repulsive forces only at high speeds with *large* guideway clearances of 10~15cm. As for the EMS system, it can lift a train up to 8~10mm using attractive forces by the distributed magnets beneath a guide-rail at any speed, which is the major

---

[1] Corresponding author: Department of Architecture, Tamkang University, Taipei 10620, Taiwan, e-mail: jdyau@mail.tku.edu.tw

difference from the EDS system.

From the past literatures in dynamics of maglev vehicle/guideway system, Cai and his co-workers (1995-97) investigated the response characteristics of different maglev vehicle models traveling over flexible guideways. They concluded that a concentrated-load vehicle model might result in larger responses of both guideway deflections and vehicle accelerations than a distributed-load vehicle model. In the literature review works conducted by Cai and Chen (1997), various aspects of the dynamic characteristics, magnetic suspension systems, vehicle stability, suspension control laws for maglev and guideway coupling systems were discussed. Zheng et al. (2000; 2005) presented two kinds of vehicle/guideway coupling models with controllable magnetic suspension systems to investigate the vibration behavior of a maglev vehicle running on a flexible guideway. They observed the phenomena of divergence, flutter, and collision on the dynamic stability of a maglev-vehicle traveling on a flexible guideway.

In this study, a maglev vehicle is simulated as a rigid car body connecting a rigid magnetic bogie-set with a uniformly distributed spring-dashpot system and the aerodynamic forces acting on the moving vehicles are modeled as quasi-steady wind loading with mean speeds. Based on maglev theory, the maglev system is lifted up above the guideway with stable levitation gaps via motion-dependent electromagnetic forces. By employing Galerkin's method to convert the governing equations of a moving maglev vehicle into a set of generalized differential equations, the computation of dynamic response for the vehicle system was carried out using an iterative approach with Newmark's method (Newmark, 1959). To provide suitable control gains in tuning the magnetic force in the maglev suspension system for the dynamic response of the maglev vehicle moving at various speeds, an on-board PI controller based on Ziegler-Nicholas (Z-N) method (Astrom and Hagglund, 1988; Ogata, 1997) is used in the maglev system. Numerical simulations demonstrate that the aerodynamic forces play an important role in amplifying the acceleration amplitude of the running maglev vehicle as a result of increasing the moving speeds.
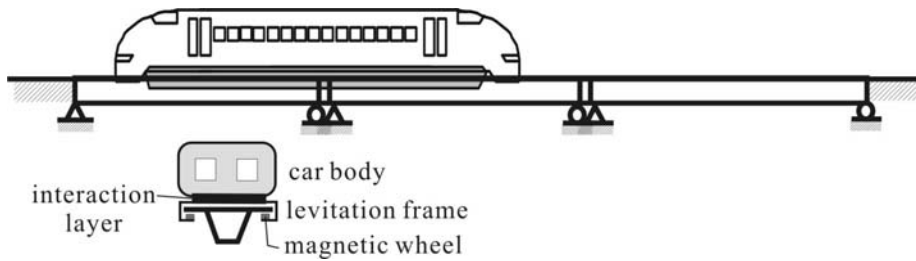


**Fig. 1. Schematic diagram of a running EMS vehicle.**
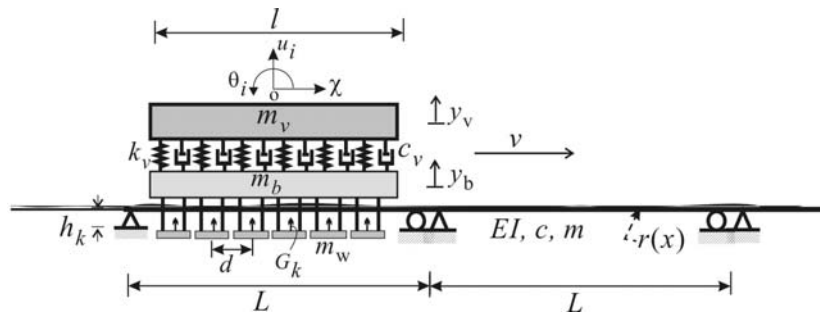


**Fig. 2. Mathematical model of a moving maglev vehicle.**

# PROBLEM FORMULATION

From the numerical results presented by Cai et al. (Cai et. al., 1995-97), they pointed out that a distributed-load vehicle model behaves better than a concentrated-load model in both responses of guideway and vehicles, which indicates that the vehicle supported with multiple magnets may have better ride quality. For this reason, the maglev vehicle supported with multiple magnetic wheels is employed to conduct the dynamic behavior of a moving maglev vehicle illustrated in this study. As shown in Fig. 1, an EMS-type maglev vehicle model is traveling over a rigid guideway system. Considering the dominant factor for vibration behaviors of the maglev vehicle system, only vertical motions of the dynamic model are concerned in this study (Cai et al., 1996; Yau, 2009).

Since this paper is regarded as a preliminary research of theoretical development for a traveling maglev vehicle with the inclusion of aerodynamic forces, some basic assumptions are adopted as follows: (1) The maglev vehicle is simulated as a rigid double-beam system, in which the car body and the magnetic bogi-set are modeled as two rigid parallel beams connected by an interaction layer using a uniformly distributed spring-dashpot system (see Fig. 2); (2) Allowable levitation gap ($h$) at the magnetic wheel does not contact with the guide rail, i.e., $h > 0$; (3) The magnetic wheels are regarded as a series of equal-distant concentrated masses attached to the rigid bogie-set; (4) The effect of time delay between the input voltage and the output current on the maglev suspension system is negligible; (5) Only the mean aerodynamic forces of lift and pitching moment at quasi-steady state is considered as the magelv vehicle travels at high speeds, that is, the aerodynamic effect of turbulent flow is neglected in this study; (6) The wind forces acting on both the maglev vehicle and guideway girders are assumed to be negligible; (7) The aerodynamic forces acting on the guideway girder are regarded so small that their dynamic effects can be neglected.

### Governing equations of motion

As shown in Fig. 2, a maglev vehicle supported by multiple magnet wheels with equal-intervals ($d$) is passing through a series of simple beams at constant speed $v$. Here, we shall use the following symbols to denote the properties depicted in the schematic diagram of Fig. 2: $m$ = distributed mass of the beam, $c$ = damping coefficient, $EI$ = flexural rigidity, $l$ = car length, $m_w$ = lumped mass of magnetic wheel, $m_b$ = distributed mass of the levitation frame, $m_v$ = distributed mass of the car body, and $(u_i, \theta_i)\big|_{i=b,v}$ = midpoint displacement and rotation components of the rigid-double beam system. Here, the subscripts $b$ and $v$ are denoted as the rigid lower beam (levitation frame) and upper beam (car body) for the EMS-type maglev vehicle model, respectively. With the inclusion of ground settlement at guideway supports, one can formulate the equation of motion for the $j$th guideway girder carrying a moving maglev vehicle suspended by multiple magnetic forces $G_k$ as follows (Yau, 2009):

$$m\ddot{u}_j + c\dot{u}_j + EIu_j'''' = \sum_{k=1}^{K}\left[G_k(i_k, h_k)\varphi_j(x,t)\right],$$
$$\varphi_j(x,t) = \delta\left(x - x_k\right)\left[H\left(t - t_k - \frac{(j-1)L}{v}\right) - H\left(t - t_k - \frac{jL}{v}\right)\right], \tag{1}$$

together with the following non-homogeneous boundary conditions due to vertical support movements:

$$u_j(0,t) = u_j(L,t) = EIu_j''(0,t) = EIu_j''(L,t) = 0, \tag{2}$$

where $(\bullet)' = \partial(\bullet)/\partial x$, $(\bullet) = \partial(\bullet)/\partial t$, $u_j(x,t)$ = vertical deflection of the $j$th span, $L$ = span length, $K$ = number of magnetic wheel-sets attached to the rigid levitation frame, $\delta(\bullet)$ = Dirac's delta function, $H(t)$ = unit step function, $k = 1, 2, 3, \ldots, K$th moving magnetic wheel on the beam, $t_k = (k - 1)d/v$ = arrival time

of the $k$th magnetic wheel into the beam, and $x_k$ = position of the $k$-th magnetic wheel on the guideway. By considering aerodynamic lift force and pitching moment, the equations of motion for a 4-DOF maglev vehicle are given as:

**Lower Beam (levitation frame):**

$$(m_b l + K m_w)\ddot{u}_b + c_v l(\dot{u}_b - \dot{u}_v) + k_v l(u_b - u_v) = -f_0 l + F_y + \sum_{k=1}^{K}\left[G_k(i_k, h_k)\right],$$

$$I_{bT}\ddot{\theta}_v + \frac{l^2}{12}\left[c_v(\dot{\theta}_v - \dot{\theta}_b) + k_v(\theta_v - \theta_b)\right] = M_z + \sum_{k=1}^{K}\left[G_k(i_k, h_k)d_k\right], \tag{3}$$

**Upper Beam (car body):**

$$m_v\ddot{u}_v + c_v(\dot{u}_v - \dot{u}_b) + k_v(u_v - u_b) = 0,$$

$$I_v\ddot{\theta}_b + \frac{l^2}{12}\left[c_v(\dot{\theta}_b - \dot{\theta}_v) + k_v(\theta_b - \theta_v)\right] = 0, \tag{4}$$

in which $d_k$ = distance of the $k$th magnetic wheel to the midpoint of the lower beam, $I_{bT} = m_b l^2/12 + \sum_{k=1}^{K} m_w d_k^2$ = total moment of inertia for the rigid levitation frame, $I_v = m_v l^2/12$ = moment of inertia for the rigid car body, and $f_0 = (m_v + m_b + K m_w/l)g$ = average weight per unit length. Eq. (3) represents the equations of motion for the levitation frame interacting with the guideway and Eq. (4) for the rigid car body. Besides, from the condition of static equilibrium for the suspended maglev vehicle, one can obtain the following *static* electromagnetic force at the $k$th magnetic wheel from Eq. (3)

$$G_k(i_0, h_0) = \kappa_0\left(i_0/h_0\right)^2 = f_0 l/K, \quad \kappa_0 = f_0 l\left(h_0/i_0\right)^2/K. \tag{5}$$

**Control Equation of the maglev system**

By the theory of electromagnetic circuits, the electromagnetic equation of magnet current and control voltage for the $k$th magnetic wheel in the magnetic suspension system is given by (Sinha, 1987)

$$\Gamma_0\frac{d(i_k/h_k)}{dt} + R_0 i_k = V_k, \tag{6}$$

where $\Gamma_0 = 2\kappa_0$ = initial inductance of the coil winding the suspension magnet, $R_0$ = coil resistance of electronic circuit, and $V_k$ = control voltage. To observe the dynamic response of a moving mgalev vehicle system, this study will only consider the PI controller with *constant* tuning gains for a specific desired air gap. The control voltage of $V_k$ can be expressed using PI tuning algorithm as (Astrom and Hagglund, 1988; Ogata, 1997; Yau, 2009)

$$V_k = K_p e_k + K_i\int_0^t e_k dt, \tag{7}$$

where $K_p$ = proportional gain and $K_i$ = integral gain. Let us adopt the variable transformation as $\gamma_k = i_k/h_k$, and the error function of $e_k = i_0/h_0 - i_k/h_k = \gamma_0 - \gamma_k$ in the control process. Then substituting Eq. (7) into Eq. (6) and differentiating this equation with respect to time, after some mathematical manipulation, one can achieve the following differential equation for control error function

$$\Gamma_0 \ddot{e}_k + (K_p + R_0 h_k)\dot{e}_k + (K_i + R_0 \dot{h}_k)e_k = R_0 \gamma_0 \dot{r}(x_k) + R_0 \gamma_0 (\dot{u}_b + d_k \dot{\theta}_b). \tag{8}$$

With the aid of control error function $e_k$ and $\gamma_0 = i_0/h_0$ defined previously, the equations of motion in Eqs. (3) and (4) for an EMS maglev vehicle are rewritten as (Yau, 2009)

$$
\begin{aligned}
&(m_b l + K m_w)\ddot{u}_b + c_v l(\dot{u}_b - \dot{u}_v) + k_v l(u_b - u_v) + \frac{2f_0 l}{\gamma_0 K}\sum_{k=1}^{K} e_k = F_y + \frac{f_0 l}{K\gamma_0^2}\sum_{k=1}^{K} e_k^2, \\
&I_{bT}\ddot{\theta}_v + \frac{l^2}{12}\left[c_v(\dot{\theta}_v - \dot{\theta}_b) + k_v(\theta_v - \theta_b)\right] + \frac{2f_0 l}{\gamma_0 K}\sum_{k=1}^{K}(d_k e_k) = \frac{f_0 l}{K\gamma_0^2}\sum_{k=1}^{K}(d_k e_k^2), \\
&m_v\ddot{u}_v + c_v(\dot{u}_v - \dot{u}_b) + k_v(u_v - u_b) = 0, \\
&I_v\ddot{\theta}_b + \frac{l^2}{12}\left[c_v(\dot{\theta}_b - \dot{\theta}_v) + k_v(\theta_b - \theta_v)\right] = 0,
\end{aligned}
\tag{9}
$$

The solution of the nonlinear and coupled equations in Eqs. (8) and (9) can yield the dynamic response of the maglev vehicle moving at constant speeds. An incremental-iterative procedure needs to be carried out in dynamic analysis of maglev vehicle/guideway coupling system.


**Genralized equations of guideway girders**

The response of *dynamic* deflection $u(x,t)$ in Eq. (1) associated with the homogeneous boundary conditions in Eqs.(2) can be solved by Galerkin's method (Yang et al., 2004; Yau, 2009) and computed by Newmark's method (Newmark, 1959) in the time domain. According to the homogeneous boundary conditions shown in Eqs. (2), the dynamic deflection ($u_{dj}$) of a simple beam can be approximated by (Yau, 2009):

$$u_j(x,t) = \sum_{n=1} q_{jn}(t)\sin\frac{n\pi x}{L} \tag{10}$$

where $q_{jn}(t)$ means the generalized coordinate associated with the $n$th assumed mode of the $j$th span. First, multiplying both sides of Eq. (1) with respect to the variation of the dynamic deflection, and then integrating the equation over the beam length $L$, one can obtain the following generalized equation of motion for the $n$th *dynamic* system of the $j$th beam:

$$m\ddot{q}_{jn} + c\dot{q}_n + k_n q_{jn} = p_{jn}, \tag{11}$$

where $k_n = EI(n\pi/L)^4$ = generalized stiffness, and the generalized magnetic force is

$$
\begin{aligned}
&p_{jn} = \frac{2}{L}\sum_{k=1}^{K}\left[G_k(i_k, h_k)\times\psi_{jn}(\varpi_n, t)\right], \\
&\psi_{jn}(\varpi_n, t) = \sin\varpi_n(t-t_k)\left[H(t-t_k - \frac{(j-1)L}{v}) - H\left(t-t_k - \frac{jL}{v}\right)\right],
\end{aligned}
\tag{12}
$$

with $\varpi_n = n\pi v/L$ (Yang et al., 2004; Yau, 2009).
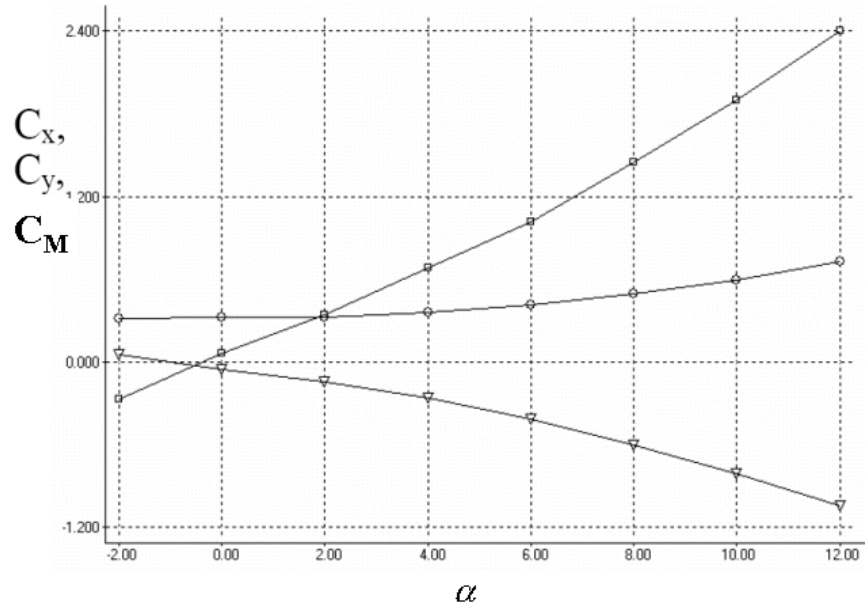
**Fig. 3. Relations between drag coefficient (○- C_x), lift coefficient (□- C_y), pitching moment (△ - C_M ) from angle of attack α. (Prykhodko et al.)**

**Aerodynamic forces on the moving maglev vehicle**

Since only the vertical and pitching vibrations of the beam are concerned, the lateral vibration of the beam caused by aerodynamic drag force will be ignored. The *aerodynamic lift force* $F_y$ and *pitching moment* $M_z$ acting on the running vehicle can be expressed as function of aerodynamic coefficients in terms of angle of attack ($\alpha$) as follows (Prykhodko et al.):

$$F_y = \frac{\rho S v^2}{2} C_y(\alpha), \quad M_z = \frac{\rho S v^2 h_v}{2} C_M(\alpha), \tag{13}$$

where $\rho$ = the air density, $\alpha$ = angle of attack, $S$ = vehicle frontal area, $h_v$ = reference heigh, $C_y$ = aerodynamic lift coefficient, and $C_M$ = aerodynamic pitching moment coefficient. As indicated in Fig. 3, the *aerodynamic coefficient curves* established by experimental means are nonlinear functions of angle of attack $\alpha$, which were obtained with the mean components given by Prykhodko et al. Here, the aerodynamic coefficient curves are first approximated by a number of *piecewise connected linear segments* through subdivision and then calculated using an interpolation method after the pitching rotation of the vehicle response has been computed. With this, an incremental-iterative approach can be employed to analyze the time history response of the bridge under the simultaneous action of the train and wind loads.

## INCREMENTAL-ITERATIVE APPROACH

Due to the motion-dependent nature of control electromagnetic forces and velocity-dependent characteristics of aerodynamic forces, the nonlinear dynamic analysis of the maglev vehicle system needs to be solved by iterative method. As shown in the analysis flowchart of Fig. 4, the procedure of incremental iterative for nonlinear dynamic analysis involves three phases: *predictor*, *corrector*, and

*equilibrium checking* (Yau, 2009). In this paper, the root mean square of the sum of the unbalanced forces for the moving maglev vehicle system is larger than preset tolerance (say $10^{-3}$) iteration for removing the unbalanced forces involving the two phases of predictor and corrector should be repeated. As indicated in previous section, the aerodynamic coefficient curves are approximated by a number of *piecewise connected linear segments* through subdivision and calculated using an interpolation method after the pitching rotation of the vehicle response has been computed by an iterative procedure for extracting the unbalanced force from the maglev-vehicle/guideway coupling system.
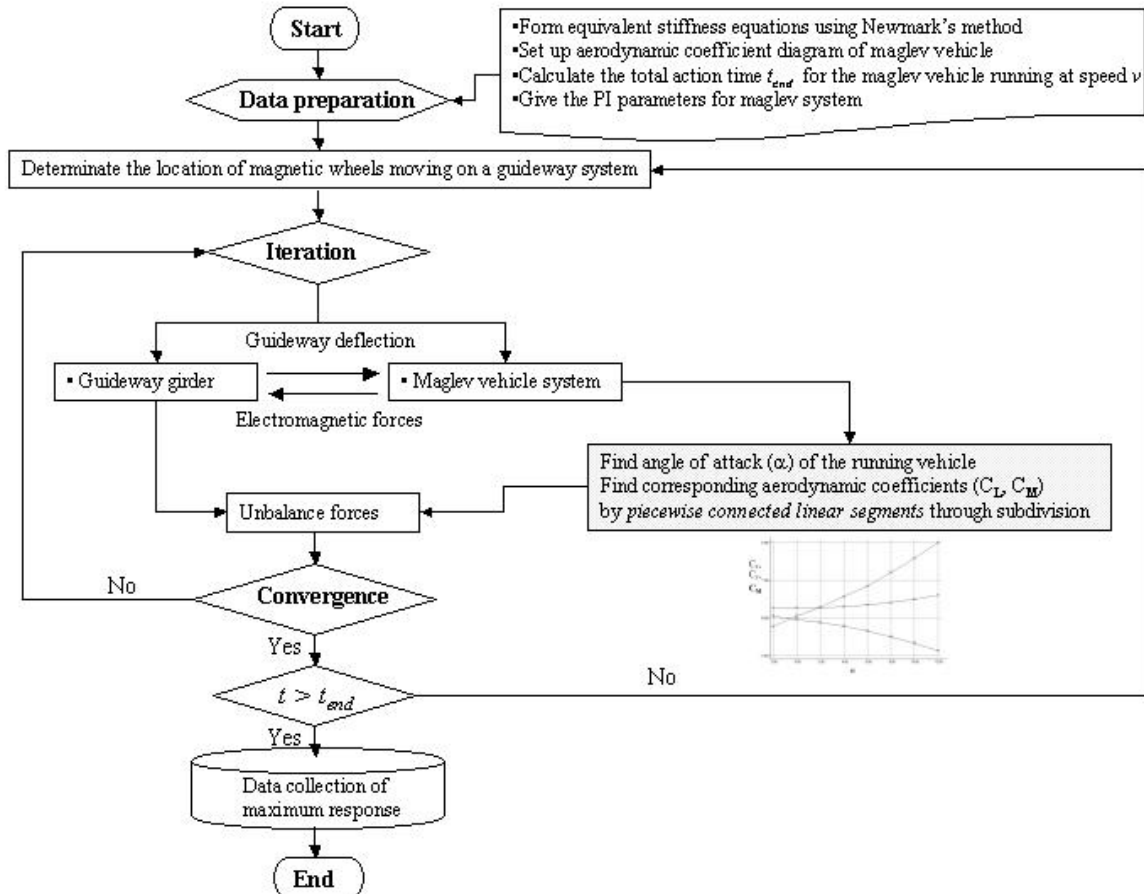


**Fig. 4. Flow chart of dynamic analysis.**

**Table 1. Properties of the guideway girder**

| L (m) | EI (kN m$^2$) | m (t/m) | c (kN-s/m/m) | $f_1$ (Hz) |
|---|---|---|---|---|
| 25 | 2.5x10$^7$ | 3.76 | 15.4 | 6.5 |

**Table 2. Properties of the maglev vehicle**

| L (m) | K | $m_b$ (kg/m) | $m_v$ (kg/m) | $m_w$ (kg) | $c_v$ (N s/m) | $k_v$ (N/m) | $i_0$ ($\Omega$) | $R_0$ (A) |
|---|---|---|---|---|---|---|---|---|
| 25 | 8 | 1200 | 600 | 200 | 4.1x10$^3$ | 7.5x10$^3$ | 25 | 1.0 |

**Table 3. Optimal PI parameters based on Z-N tuning rule**

| $h_0$ (m) | $K_{cr}$ | $T_{cr}$ (s) | $K_p$ (= 0.45$K_{cr}$) | $K_i$ (= 0.54$K_{cr}$/$T_{cr}$) |
|---|---|---|---|---|
| 0.030 | 0.095 | 0.15 | 0.043 | 0.34 |

## NUMERICAL EXAMPLES

Figure 2 shows a maglev vehicle is traveling over a series of guideway girders with identical spans at constant speed $v$. The properties of the guideway girder and maglev vehicle are listed in Tables 1 and 2, respectively. Table 3 is the list of optimal PI parameters based on Z-N tuning rules for the on-board controller, from which the critical proportional gain $K_{cr}$ and critical period $T_{cr}$ have been obtained by Yau (2009). The time step of 0.001s and the traveling distance of 300m (12 spans) are employed to compute the dynamic response of the traveling maglev vehicle. In addition, to account for the random nature and characteristics of guide-rail irregularity in practice, the following *power spectrum density* (PSD) function (Yang et al., 2004) is given to simulate the vertical profile of track geometry variations

$$S(\Omega) = \frac{A_v \Omega_c^2}{(\Omega^2 + \Omega_r^2)(\Omega^2 + \Omega_c^2)},\tag{14}$$

where $\Omega$ = spatial frequency, and $A_v$, (= $1.5 \times 10^{-7}$ m), $\Omega_r$ (= $2.06 \times 10^{-6}$ rad/m), and $\Omega_c$ (= 0.825 rad/m) are relevant parameters. In the following examples, the traveling speeds of the maglev vehicle are ranged from 100 km/h to 700km/h with an increment of 5km/h.
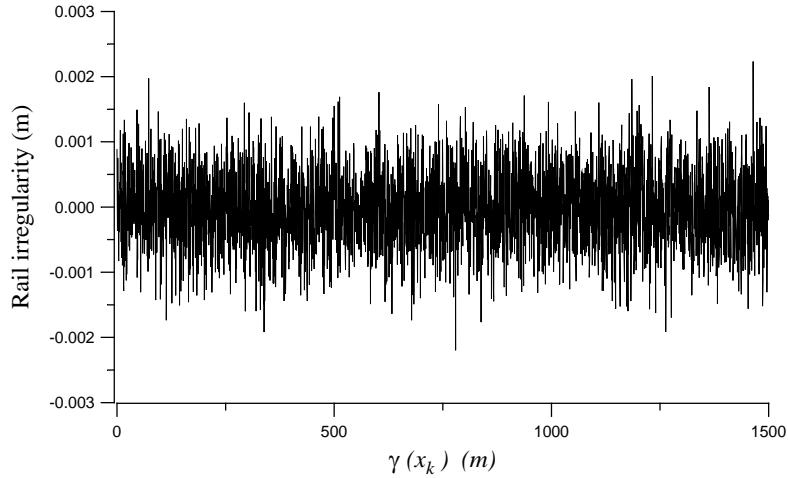


**Fig. 5. Rail irregularity (vertical profile).**

**Maximum response analysis**

Consider the optimal PI parameters listed in Table 3, which was obtained from Yau (2009). Let us define the maximum vertical acceleration compued herein as follows:

$$a_{v,\max} = \max\left(\left|\ddot{u}_v + d_k \ddot{\theta}_v\right|_{k=1,2,\dots,K}\right)\tag{15}$$

Figure 6 depicts the maximum vertical acceleration ($a_{v,max}$) of the rigid car body against the speeds. Such a relationship is denoted as $a_{v,max}$–$v$ plot in the following. As can be seen, the acceleration amplitude of the

maglev vehicle increases along with the increase of running speeds. In addition, Fig. 7 depicts the corresponding maximum response ($a_{max}$) of midspan acceleration at the departure guideway girder. The relationship between $a_{ma}$ and moving speed $v$ is called as $a_{v,max}$–$v$ plot in the following. As the plot indicated, the maximum acceleration of midspan of the guideway girder also increases with the increase of moving speeds.

**Effect of aerodynamic forces**

For the purpose of illustration, let us consider the aerodynamic coefficients of lift and pitching moment shown in Fig. 3. With the incremental iterative procedure previously, the corresponding $a_{v,max}$–$v$ plot and $a_{max}$–$v$ plot for the maglev vehicle and the midpoint of the departure guideway girder have been drawn in Figs. 6 and 7, respectively. As indicated in Fig. 6, the inclusion of aerodynamic forces has generally amplified the response of the running maglev vehicle, especially for the higher speeds over 600km/h. Moreover, the results show that the $a_{max}$-$v$ plots in Fig. 7 for the moving speeds lower than 600km/h are almost identical. One of the reasons is that the inertial force and aerodynamic effect induced by the running maglev vehicle acting on the guideway girder is much smaller than the *static* weight of the vehicle. But as the maglev vehicle moves on the guideway over 600km/h, the effects of inertial and aerodynamic forces acting on the vehicle will become rather significant on the guideway response.
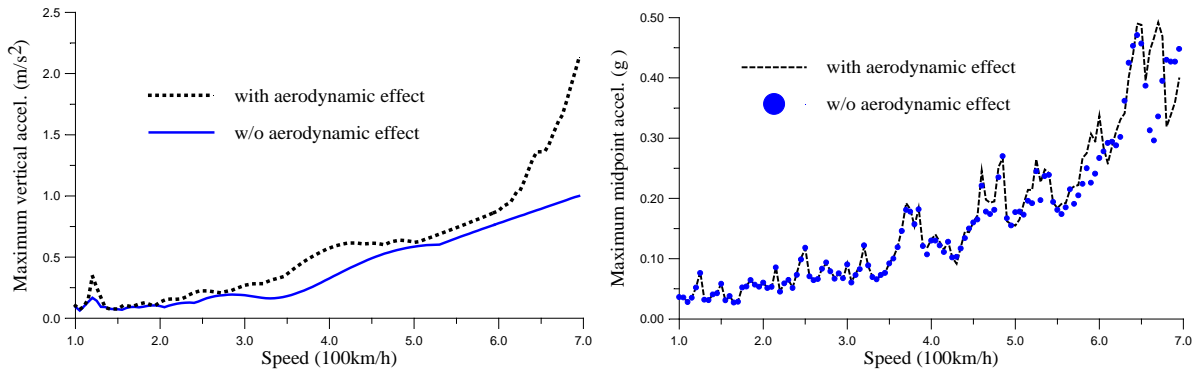


Fig. 6. $a_{v,max}$-$v$ plot of the maglev vehicle.   Fig. 7. $a_{max}$-$v$ plot of departure span of the guideway.

# CONCLUSION

Considering the quasi-static aerodynamic lift and pitching moment acting on a running EMS-type maglev evhicle, the nonlinear dynamic analysis for the vehicle installed with an on-board PI controller was carried out using an incremental-iterative procedure involving three phases: *predictor, corrector,* and *equilibrium checking*. Based on the present study, some observations are drawn as follow: (1) The numerical examples demonstrate that the proposed PI controller based on Z-N tuning method can reasonably control the maglev system for the EMS-type maglev vehicle moving at high speeds; (2) The maximum acceleration amplitude of the moving maglev vehicle is significantly amplified with the increase of moving speeds; (3) The aerodynamic forces play an important role in affecting the interaction response of maglev-vehicle/guideway system due to their velocity-dependent characteristics, especially for the higher speeds over 600km/h. Such a phenomenon should be taken into account in the stage of analysis and design of high speed maglev transport system; (4) From the practical viewpoint of operating maglev vehicles, the inclusion of cross wind forces with turbulent flow is necessary to be carried out in future study.

## ACKNOWLEDGMENTS

## REFERENCES

Astrom, K.J., and T. Hagglund (1988), Automatic Tuning of PID Controllers, Instrument Society of America.

Bittar, A. and R. M. Sales (1998), H2 and H∞ control for maglev vehicles, IEEE Control Systems Magazine 18(4), 18-25.

Cai, Y. and S.S. Chen (1995), Numerical analysis for dynamic instability of electrodynamic maglev systems, Shock and Vibration 2, 339–349.

Cai, Y., S.S. Chen, D.M. Rote, H.T. Coffey (1996), Vehicle/guideway dynamic interaction in maglev systems, ASME, Journal of Dynamic Systems, Measurement, and Control 118, 526–530.

Cai, Y. and S.S. Chen (1997), Dynamic characteristics of magnetically-levitated vehicle systems, ASME, Appl. Mech. Rev. 50(11), 647–670.

Newmark, N.M. (1959), A method of computation for structural dynamics, Journal of Engineering Mechanics Division, ASCE 85, 67–94.

Ogata, K. (1997) Modern Control Engineering, 3rd ed., Prentice-Hall Intl. Inc., N.J.

Poulin, E. and A. Pomerleau (1999), PI settings for integrating processes based on ultimate cycle information, IEEE Transactions on Control Systems Technology 7(4), 509-511.

Prykhodko, O.A., A.V. Sohatsky, O.B. Polevoy, and A.V. Mendriy, Computational and wind tunnel experiment in high-speed ground vehicle aerodynamics.

Sinha, P.K. (1987), Electromagnetic Suspension, Dynamics and Control, Peter Peregrinus Ltd., London, U.K.

Yang, Y.B., J.D. Yau, and Y.S. Wu (2004), Vehicle-Bridge Interaction Dynamics, World Scientific.

Yau, J.D. (2009), Response of a maglev vehicle moving on a series of guideways with differential settlement, J. Sound & Vibration, 324(3-5), 816-831.

Zheng, X.J., J.J. Wu, and Y.H. Zhou (2000), Numerical analyses on dynamic control of five-degree-of-freedom maglev vehicle moving on flexible guideways, Journal of Sound and Vibration 235, 43–61.

Zheng, X.J., J.J. Wu, and Y.H. Zhou (2005), Effect of spring non-linearity on dynamic stability of a controlled Maglev vehicle and its guideway system, Journal of Sound and Vibration 279, 201–215.